


RESEARCH

Open Access



# Biosynthesis, characterization, and antibacterial activity of ZnO nanoaggregates using aqueous extract from *Anacardium occidentale* leaf: comparative study of different precursors

Eric Kwabena Droepenu<sup>1,2\*</sup> , Ebenezer Aquisman Asare<sup>1,2</sup>, Boon Siong Wee<sup>1\*</sup>, Rafeah Binti Wahi<sup>1</sup>, Frederick Ayertey<sup>4</sup> and Michael Odoi Kyene<sup>3</sup>

## Abstract

**Background:** Various parts of *Anacardium occidentale* plant possess curative qualities like antidiabetic, anti-inflammatory, antibacterial, antifungal, and antioxidant. Aqueous extract of this plant leaf was used in biosynthesizing zinc oxide (ZnO) nanoaggregates using two precursors of zinc salt (zinc acetate dihydrate  $[\text{Zn}(\text{CH}_3\text{COO})_2 \cdot 2\text{H}_2\text{O}]$  and zinc chloride  $[\text{ZnCl}_2]$ ). The synthesized ZnO samples were used in a comparative study to investigate the antibacterial activity against selected Gram-positive and Gram-negative microbes [*Staphylococcus aureus*, *Exiguobacterium aquaticum* (Gram +ve) and *Escherichia coli*, *Klebsiella pneumoniae*, *Acinetobacter baumannii* (Gram -ve)]. The synthesized ZnO nanoaggregates from the two precursors were characterized using Fourier transform infrared spectroscopy (FT-IR), scanning electron microscopy (SEM), transmission electron microscopy (TEM), and energy-dispersive x-ray spectroscopy (EDX) techniques.

**Results:** Micrographs of SEM and TEM confirmed nanoparticles agglomerated into aggregates. While spherical nanoaggregates were identified in samples prepared from  $\text{Zn}(\text{CH}_3\text{COO})_2 \cdot 2\text{H}_2\text{O}$ , flake-like structures were identified in samples synthesized from  $\text{ZnCl}_2$ . Particle size determined by TEM was  $107.03 \pm 1.54$  nm and  $206.58 \pm 1.86$  nm for zinc acetate dihydrate and zinc chloride precursors respectively. ZnO nanoaggregate synthesized using zinc acetate as precursor gave higher antibacterial activity than its counterpart, zinc chloride with *K. pneumonia* recording the highest inhibition zone of  $2.08 \pm 0.03$  mm (67.53%) whereas *S. aureus* recorded the least inhibition zone of  $1.06 \pm 0.14$  mm (34.75%) for ZnO nanoaggregate from zinc chloride precursor. Also, antibacterial activity increases with increasing concentration of the extract in general. However, *A. baumannii*, *E. aquaticum*, and *K. pneumoniae* did not follow the continuity trend with regards to the 250 ppm and 500 ppm concentrations.

(Continued on next page)

\* Correspondence: [kobladdodzie01@yahoo.co](mailto:kobladdodzie01@yahoo.co); [swboon@unimas.my](mailto:swboon@unimas.my)

<sup>1</sup>Resource Chemistry Program, Faculty of Resource Science and Technology, Universiti Malaysia Sarawak, 94300 Kota Samarahan, Sarawak, Malaysia  
Full list of author information is available at the end of the article

(Continued from previous page)

**Conclusion:** Biosynthesis of ZnO nanoaggregates using aqueous extract of *A. occidentale* leaf from zinc acetate dihydrate and zinc chloride as precursors was successful with the formation of nanospheres and nanoflakes. The study suggested that *A. occidentale* sp. could be an alternative source for the production of ZnO nanoparticles and are efficient antibacterial compounds against both Gram +ve and Gram -ve microbes with its promising effect against infectious bacteria.

**Keywords:** Zinc oxide nanoaggregate, Zinc acetate dihydrate, Zinc chloride, *Anacardium occidentale*, Antibacterial activity, Biosynthesis

## 1 Background

Nanotechnology is a growing field of study combining technology, bio-nanoscience, and material science together [1]. Serious interests arose in the last few decades among scientists into some unique properties: catalytic, magnetic, electronic, optical, antibacterial, antimicrobial, anti-inflammatory, and wound healing of nanoparticles [2–4]. When different precursors are used in the synthesis of ZnO particles at different reaction conditions (reaction time, concentration, and temperature), literature shows that different morphologies, such as flower shape and needle shape, are produced with different sizes [5–7]. The porosity of the synthesized nanoparticles enhances the surface area and chemical and photochemical stability [8, 9]. Research has also shown that ZnO nanoparticles synthesized biologically have shown strong antibacterial effect than those synthesized through chemical means [10, 11]. The type of plant extract and its concentration used in a biosynthesis reaction have an effect on the morphology of ZnO nanoparticles. For instance, extract containing functional groups such as alcohol, ketone, carboxylic acid, and amine creates spherical-shaped ZnO nanoparticles, whereas extract with -OH (hydroxyl) group gives quasi-spherical agglomerates [12, 13].

Natural products such as chitosan and extracts of fungi, bacteria, and different plant genus extracts are used as stabilizing and reducing agents which serve as alternative to chemical synthesis of nanoparticles [14]. The reason has been reported to be due to the fact that green synthesis of nanoparticles is environmentally favorable, simple, economical, and comparatively reproducible. The concentration of metabolites in the plant extracts, pH, as well as the temperature used in the plant extract preparation has an effect on the morphology of the nanoparticles to be formed [15–19]. ZnO nanoparticles are known to be one of the multipurpose inorganic nanoparticles with effective antibacterial, antimicrobial, and antifungal activities [20] even at very low concentrations.

*Anacardium occidentale* (cashew) belongs to the genus *Anacardium* and family Anacardiaceae, which is found worldwide. The plant is predominantly grown in Dormaa Ahenkro in the Brong Ahafo region of Ghana, West

Africa, as a cash crop. Different parts of this plant species possess curative qualities like antidiabetic, anti-inflammatory, antibacterial, antifungal, and antioxidant. This was reported by different studies that investigated into these activities and has proven its viability and effectiveness [21–26].

Phytochemical constituents of this plant as investigated by Ojezele and Agunbiade [27] reported the presence of tannin = 15.38 mg/g, total polyphenolics = 2.00 mg/g, alkaloid = 39.90%, and oxalate = 8.13%. Also, Fadeyi et al. [28] identified fatty acid esters and a new androstane steroid derivative being reported for the first time. Bastos et al. [29] also in a study went further to isolate anacardic acid, cardol, and cardanol compounds from this plant to evaluate its inhibition against *Trypanosoma cruzi* Sirtuins. From their report, isolation was successful with positive inhibition against pathogens under study.

Nevertheless, literature survey reveals the synthesis of platinum nanoparticles from this plant species and its catalytic and thermal applications but with very little information on zinc oxide nanoparticle synthesis [30]. Hence, the study sort to synthesize ZnO nanocrystals from aqueous extract of *A. occidentale* from two precursors and also investigate their antibacterial activity against selected Gram-positive and Gram-negative microbes [*Staphylococcus aureus*, *Exiguobacterium aquaticum* (Gram +ve) and *Escherichia coli*, *Klebsiella pneumoniae*, *Acinetobacter baumannii* (Gram -ve)]. Aqueous extract was preferred for this study because the extraction process is simple and free from contaminants.

## 2 Methods

### 2.1 Collection and preparation of plant extracts

The plant species (*A. occidentale*) was formally identified by the two individuals of the Centre for Plant Medicine Research, Mampong-Akuapem, Ghana, who doubles as co-authors of this paper. *A. occidentale* fresh leaves were collected from a peasant farmer in Dormaa Ahenkro in the Brong Ahafo Region of Ghana, West Africa, in September 2019 upon a request. Since the plant species was meant for study purposes and not for any commercial reasons, permission was granted to harvest the leaves

without attaining any voucher specimen. The harvested fresh leaves of the plant species were brought to the phytochemical lab of the Centre for Plant Medicine Research, Mampong-Akuapem, Ghana. The fresh plant leaves were washed under running water and double-distilled water. The method reported by Droepenu and Asare [31] for aqueous plant extract preparation was adopted for this study. About  $10.0 \pm 0.1$  g of the sample (fresh leaves) was heated with 100.00 ml of distilled water at a temperature of  $60 \pm 2^\circ\text{C}$  for about 25 min. The filtrate after filtering using Whatman filter paper was stored in a clean Schott bottle for further analysis.

## 2.2 Phytochemical analysis

Preliminary qualitative phytochemical analysis was carried out on the aqueous leaf extract of *Anacardium occidentale* plant species. Fifty milliliter of the plant extract was screened for ten (10) selected phytochemical constituents as per the methods reported by Trease and Evans [32]. The phytoconstituents tested were saponins, tannins/phenolic compounds, flavonoids, reducing sugars, cyanogenic glycosides, alkaloids, triterpenes, phytosterols, anthracinosides, and polyuronides.

## 2.3 Synthesis of ZnO nanoparticles

The method reported by Moazzen et al. [33] and cited by Droepenu et al. [34] was adopted with some modifications in this study. A weighed mass of  $9.15 \pm 0.1$  g (0.05 mol) zinc acetate dihydrate  $[\text{Zn}(\text{CH}_3\text{COO})_2 \cdot 2\text{H}_2\text{O}]$  and  $6.81 \pm 0.1$  g (0.05 mol) anhydrous zinc chloride  $[\text{ZnCl}_2]$  (Sigma-Aldrich, India) was each dissolved in 50 ml of deionized water in a 250 ml Schott bottle and heated to a temperature of  $60 \pm 2^\circ\text{C}$  with constant stirring using electrical stirring hotplate (Favorit). Also,  $2.80 \pm 0.1$  g (0.05 mol) of potassium hydroxide (KOH) (VWR Amresco, USA) was dissolved in 25 ml of deionized water in a 100-ml Schott bottle under the same condition as the precursors. The KOH solutions were slowly drained dropwise from a burette into each of the  $\text{Zn}(\text{CH}_3\text{COO})_2 \cdot 2\text{H}_2\text{O}$  and  $\text{ZnCl}_2$  solutions at  $60 \pm 2^\circ\text{C}$  with vigorous stirring for an hour until white precipitate of zinc oxide was formed. Fifty milliliter of the plant extract was drained dropwise with a burette into each mixture under constant stirring at  $30 \pm 2^\circ\text{C}$  for 3 h. The solution was centrifuged at 4000 rpm for 15 min with Hanil FLETA 5 Centrifuge machine; the zinc oxide precipitate was thoroughly washed with deionized water and dried under hot air. The samples were then preserved in air-tight container for characterization and antibacterial studies.

## 2.4 Characterization of ZnO nanoparticles

Different characterization techniques were used including scanning electron microscopy (SEM) (SU3500, Hitachi) and transmission electron microscope (TEM) (JEOL

1230, Japan) in determining the morphological features of the synthesized particles. The purity and functional groups present in the synthesized ZnO nanoparticle were determined using energy dispersive x-ray spectroscopy (EDX) (JEOL 6390LA) and Fourier transform infrared spectroscopy (FT-IR) (Thermo Scientific Nicolet iS10, USA). Further assessment into the optical properties of the sample was carried out using ultraviolet visible spectroscopy (UV-vis) (UV-1800 Series, SHIMADZU) techniques. Sample preparation prior to analysis for the different characterization techniques was carried out using the method reported by Droepenu and Asare [31, 34].

## 2.5 Preparation of plant-mediated ZnO NPs test samples

The antibacterial activity of *A. occidentale*-mediated zinc oxide nanoparticles at different concentrations (25, 50, 100, 250, 500, and 1000 ppm) from the two precursors (zinc acetate dihydrate and zinc chloride) on the five selected pathogens (*Staphylococcus aureus*, *Exiguobacterium aquaticum* (Gram +ve) and *Escherichia coli*, *Klebsiella pneumoniae*, *Acinetobacter baumannii* (Gram -ve)) was determined by adopting the disc diffusion method reported by Umaru et al. [35].

## 2.6 Bacteria broth preparation

The procedure for bacteria broth preparation follows the one reported by Droepenu et al. [34] where a weighed mass of  $2.60 \pm 0.1$  g of the dried broth was dissolved (in 200 mL deionized water) and autoclave at a temperature of  $121^\circ\text{C}$ . Culture stains of the five Gram +ve and Gram -ve bacteria were obtained from the Department of Biochemistry Laboratory, University of Ghana-Legon, and incubated with a shaker at a temperature of  $37^\circ\text{C}$  [36] for 16 h. The optical density (OD) of the bacterial broth after incubation was computed by UV Mini Spectrophotometer (1240 SHIMADZU) at wavelength 575 nm and compared to the standard (0.6–0.9).

## 2.7 Inoculation of plate

Bacteria inoculation for this study follows the procedure reported by Droepenu et al. [34]. Approximately 1.0 ml of the prepared bacterial broth was streaked over the entire agar plate surface in four different directions using sterile cotton bud. A  $10 \mu\text{l}$  volume of the ZnO nanoparticle from the *A. occidentale* leaf extract from the two precursors of concentrations 25, 50, 100, 250, 500, and 1000 ppm was each pupated onto the prepared discs (6-mm diameter) and gently pressed onto the agar plate and left for 10 min at room temperature. Commercial synthesized ZnO NPs (Sigma-Aldrich, USA) containing the same volume of methanol was taken as a control to identify the activity of the solvent and ZnO nanoparticle. In addition,  $30 \mu\text{g}$  of tetracycline was used as positive

control. Each of the test samples was tested in triplicate for the bacterium used. The plate samples were then incubated at temperature of 37 °C for 24 h, and the sensitivity of the pathogenic organisms to the ZnO extracts from the two precursors were examined by the zone of inhibition around every sample disc after incubation. The inhibition zone data was computed in millimeters (mm) to show the presence of antibacterial activity for all the samples compared to the positive control and analyzed using one-way analysis of variance (ANOVA) with differences considered at  $P$  value < 0.05.

### 2.8 Drug entrapment efficiency of ZnO NPs

The entrapment efficiency of ZnO NPs was determined by an indirect method. Briefly, the precipitate of ZnO NPs from the two precursors were each separated by centrifugation at 4000 rpm for 15 min. Drug content in the supernatant was determined by measuring the absorbance using UV-Vis spectrophotometer (UV-1800 Series, Shimadzu, Japan) at 455 nm ( $\lambda$  max of extract). The amount of drug entrapped was calculated by subtracting the amount of drug in the supernatant from the total amount of drug added [37, 38]. The entrapment efficiency was calculated as follows:

$$\text{Entrapment efficiency (\%)} = \frac{\text{Amount of drug entrapped}}{\text{Total amount of drug entrapped}} \times 100\%$$

## 3 Result

### 3.1 Phytochemical analysis results

The results of the qualitative phytochemical study carried out on the aqueous leaf extract of *Anacardium occidentale* plant species is illustrated in Table 1.

### 3.2 FT-IR results

The IR spectrum analysis of the two ZnO nanoaggregates was determined at a spectral range of 4000–400  $\text{cm}^{-1}$  with resolution of 4  $\text{cm}^{-1}$  as illustrated in Fig. 1.

**Table 1** Phytochemical components of aqueous leaf extract of *Anacardium occidentale*

Constituent	Results
Saponins	+
Tannins/phenolic compounds	+
Flavonoids	+
Reducing sugars	+
Cyanogenic glycosides	
Alkaloids	+
Triterpenes	
Phytosterols	
Anthracinoides	
Polyuronides	

Before analysis, the dried powdered ZnO sample was mixed with potassium bromide (KBr) in a ratio of 1:19. The sample was then placed in the metal hole, pressed until the sample was compressed inside the hole before being used for the analysis.

### 3.3 SEM and TEM results

The SEM and TEM images of ZnO nanoaggregates from aqueous extracts of *A. occidentale* using zinc chloride and zinc acetate dihydrate as precursor are illustrated in Fig. 2a–d. Prior to analysis, the dried powdered solid ZnO sample was coated on an aluminum plate with the help of adhesive membrane for SEM analysis. In the case of TEM, the dried powdered ZnO sample was first diluted with absolute ethanol (95%) and sonicated with ultrasonic cleaner (Elma, Germany) for 10 min. A 4  $\mu\text{l}$  volume of the solution sample was loaded onto a Formvar film Copper grid (FF300-Cu) before being observed under the machine.

### 3.4 EDX results

Elemental analysis on the two ZnO nanoaggregate samples was performed by dispersive x-ray and the graph illustrated in Fig. 3 with percentage elemental composition (inset) of the graph. The same procedure used for the TEM was also carried out for the EDX analysis, but in this case, the sonicated solution was loaded onto an aluminum plate.

### 3.5 UV-vis results

The dry powdered ZnO sample was dispersed in a 95% absolute ethanol and sonicated for 10 min before the absorbance recorded using UV-1800 Series (SHIMADZU) in the range of 300–400 nm. The spectra for the two samples are illustrated in Fig. 4 a and b.

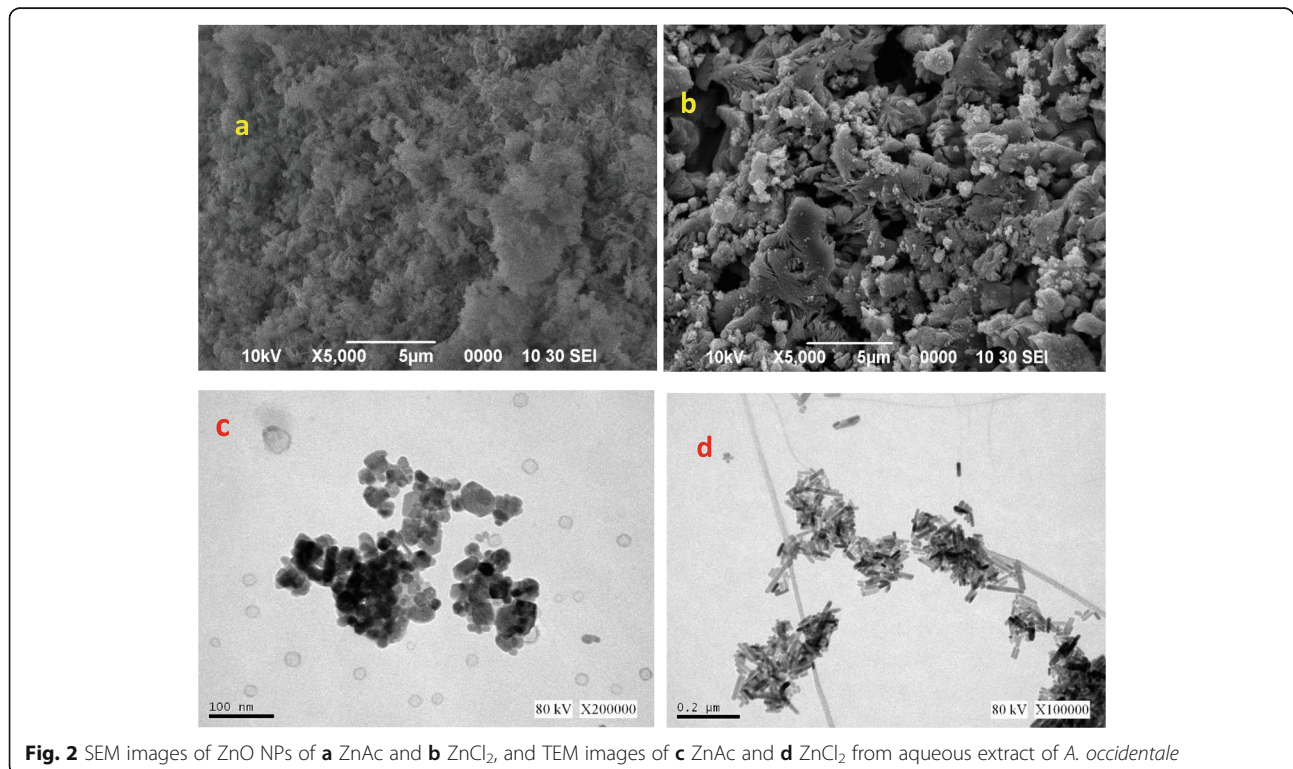
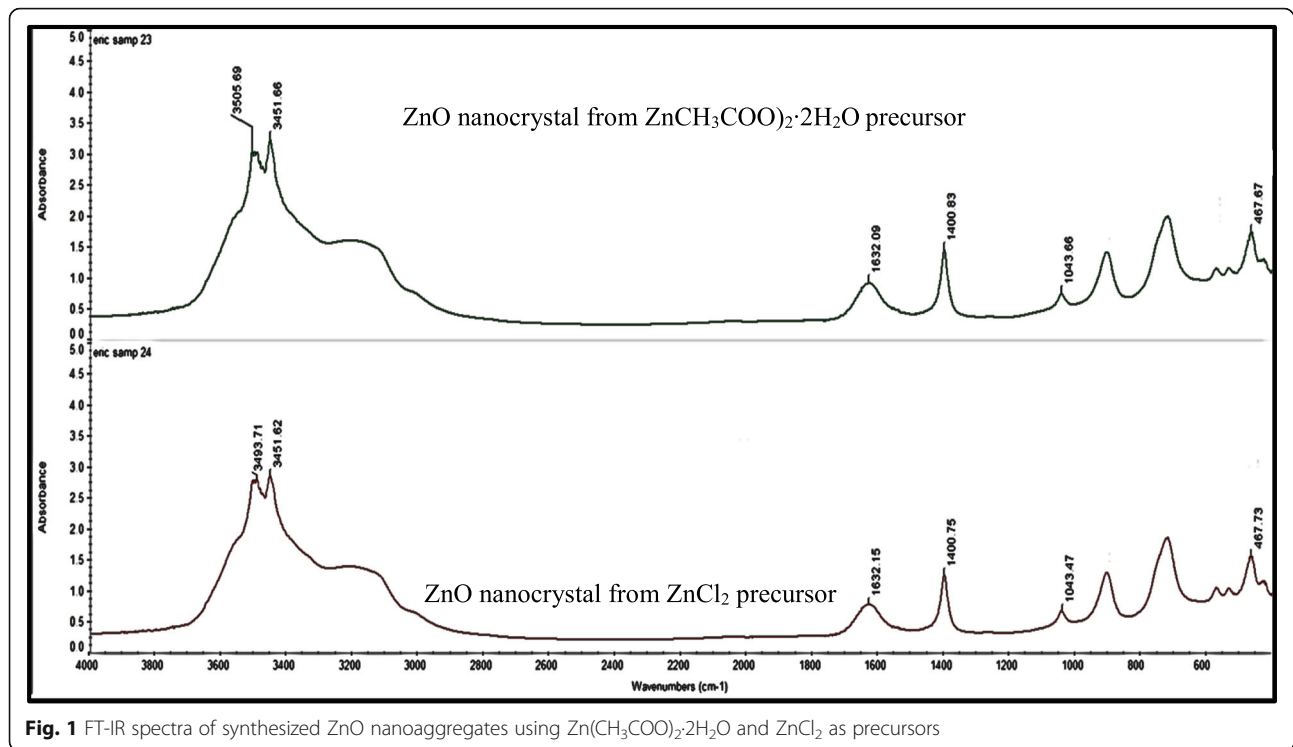
### 3.6 Antibacterial activity evaluation

The mean diameter measured for the inhibition zone and the comparison of the antibacterial activity of *A. occidentale* leaf extract-mediated biosynthesized ZnO nanoaggregates from the two precursors (zinc acetate dihydrate and zinc chloride) for the selected microbes by disc diffusion method is illustrated in Table 2 and Fig. 5 a and b.

## 4 Discussion

### 4.1 Phytochemical analysis

The aqueous leaf extract of the plant under study revealed the presence of active constituents such as alkaloids, tannins/phenolic compounds, saponins, and flavonoids. Similar study was carried out by Ojezele and Agunbiade [27], where tannins, phenolic compounds, saponins, and alkaloids were identified in the aqueous extract of the same plant species. On the other hand, *Semecarpus anacardium* L., another family of



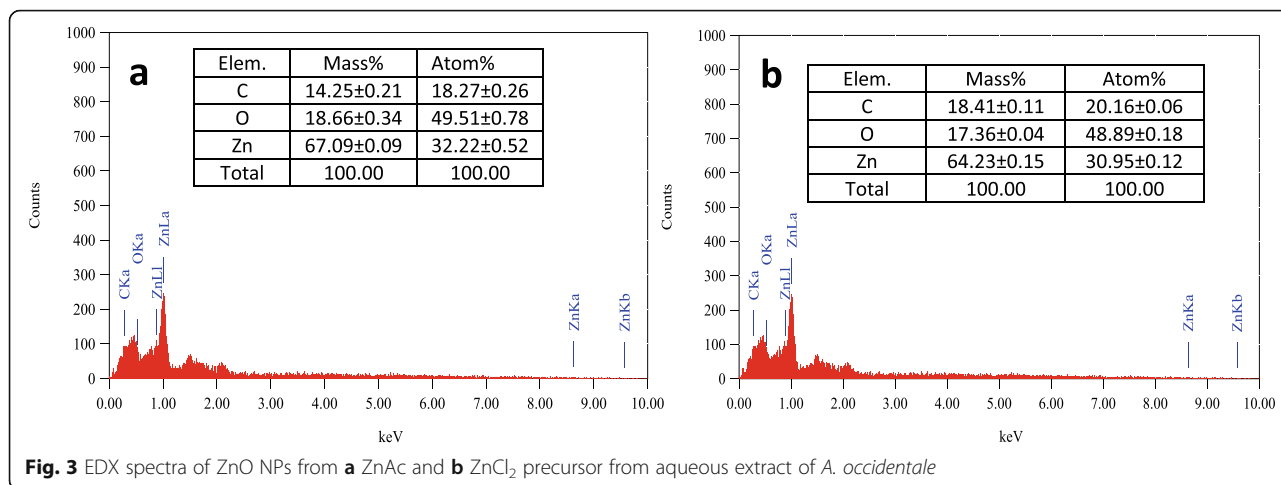


Fig. 3 EDX spectra of ZnO NPs from a ZnAc and b ZnCl<sub>2</sub> precursor from aqueous extract of *A. occidentale*

*Anacardium*, recorded the presence of steroids and terpenoids in addition to what this study found [39]. These chemical constituents are known for their medicinal activity [28].

### 4.2 FT-IR analysis

All IR spectrum peak analysis was done with reference to Socrates [40]. The spectra result shows a slight shift in the wavenumbers of the peaks which might be as a result of the precursor used to synthesize the two samples from the same plant extract.

From the spectra result of this study, the shift in the absorption bands observed at 3451.62 cm<sup>-1</sup> and 3493.71

cm<sup>-1</sup> for ZnO nanocrystals from zinc chloride precursor to 3451.66 cm<sup>-1</sup> and 3505.69 cm<sup>-1</sup> for ZnO nanocrystals from zinc acetate was identified to be the stretching vibrations of -OH groups. However, the peaks at 1632.15 cm<sup>-1</sup> (C=O), 1400.75 cm<sup>-1</sup> (C=C), and 1043.47 cm<sup>-1</sup> (C-N) for ZnO nanoaggregates from zinc chloride precursor shifted to 1632.09 cm<sup>-1</sup>, 1400.83 cm<sup>-1</sup>, and 1043.66 cm<sup>-1</sup> in the case of ZnO nanocrystals from zinc acetate dihydrate. The presence of these functional groups is a result of the constituents in the extract as indicated by literature. The corresponding wavenumber indicating ZnO stretching in the two samples is at absorption peak bands of 467.73 cm<sup>-1</sup> and 467.67 cm<sup>-1</sup> for ZnO

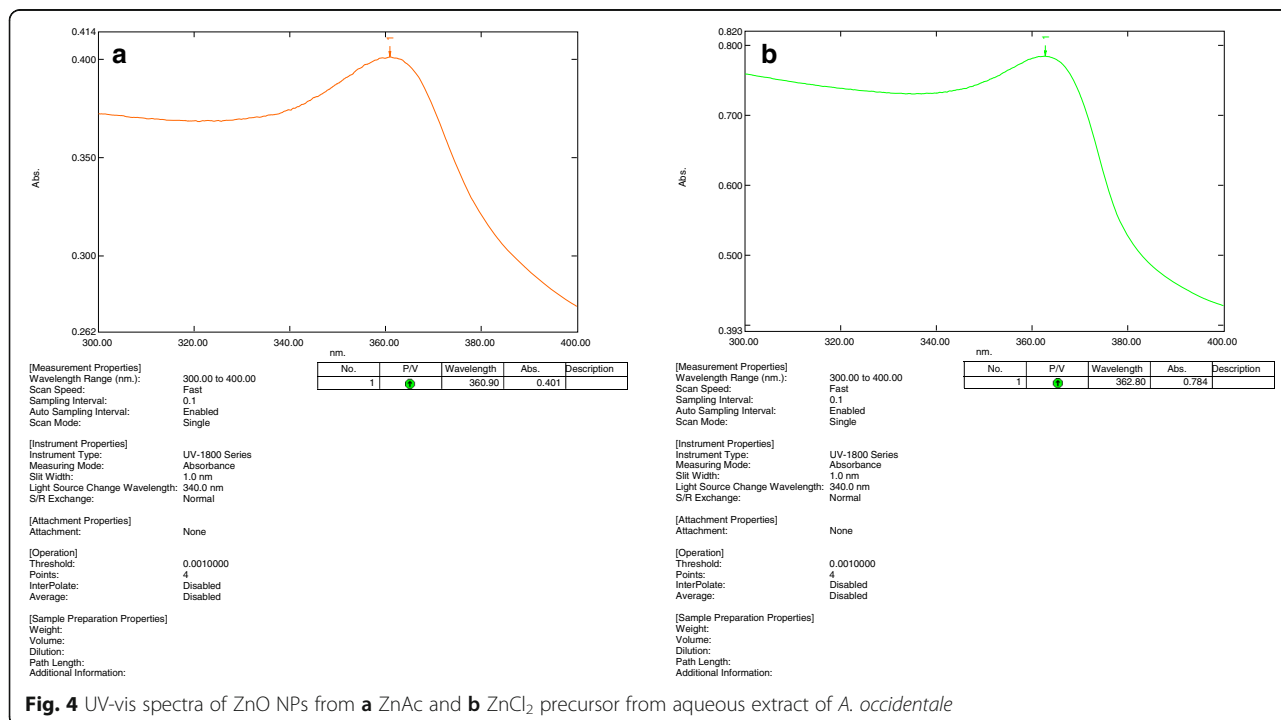


Fig. 4 UV-vis spectra of ZnO NPs from a ZnAc and b ZnCl<sub>2</sub> precursor from aqueous extract of *A. occidentale*

**Table 2** Mean inhibition zone results of *A. occidentale* leaf extract-mediated biosynthesized ZnO nanoaggregates from the two precursors against selected microbes [*S. aureus*, *E. aquaticum* (Gram positive) and *E. coli*, *K. pneumonia*, *A. baumannii* (Gram negative)]

Concentration (ppm)	ZnO NPs type	Inhibition				
		<i>E. coli</i> (Gram -ve)	<i>S. aureus</i> (Gram +ve)	<i>A. baumannii</i> (Gram -ve)	<i>E. aquaticum</i> (Gram +ve)	<i>K. pneumoniae</i> (Gram -ve)
	Control	3.06 ± 0.01 mm	3.05 ± 0.06 mm	3.07 ± 0.02 mm	3.06 ± 0.01 mm	3.08 ± 0.03 mm
25	ZnAc	1.60 ± 0.04 mm	1.49 ± 0.03 mm	1.89 ± 0.08 mm	1.61 ± 0.11 mm	1.91 ± 0.10 <sup>a</sup> mm
	ZnCl <sub>2</sub>	1.12 ± 0.04 mm	1.06 ± 0.14 mm	1.27 ± 0.13 mm	1.25 ± 0.14 mm	1.30 ± 0.22 <sup>a</sup> mm
50	ZnAc	1.68 ± 0.03 mm	1.61 ± 0.11 mm	1.90 ± 0.02 <sup>a</sup> mm	1.62 ± 0.07 mm	2.04 ± 0.15 <sup>a</sup> mm
	ZnCl <sub>2</sub>	1.13 ± 0.34 mm	1.23 ± 1.13 mm	1.29 ± 0.18 <sup>a</sup> mm	1.17 ± 0.05 mm	1.29 ± 0.12 <sup>a</sup> mm
100	ZnAc	1.69 ± 0.04 mm	1.62 ± 0.11 mm	1.79 ± 0.09 <sup>a</sup> mm	1.82 ± 0.16 mm	1.88 ± 0.02 <sup>a</sup> mm
	ZnCl <sub>2</sub>	1.23 ± 0.07 mm	1.27 ± 0.17 mm	1.24 ± 0.16 <sup>a</sup> mm	1.33 ± 0.21 mm	1.37 ± 0.16 <sup>a</sup> mm
250	ZnAc	1.78 ± 0.06 mm	1.87 ± 0.10 <sup>a</sup> mm	1.76 ± 0.05 mm	1.71 ± 0.31 mm	1.65 ± 0.17 mm
	ZnCl <sub>2</sub>	1.29 ± 0.19 mm	1.33 ± 0.15 <sup>a</sup> mm	1.30 ± 0.17 mm	1.29 ± 0.19 mm	1.30 ± 0.12 mm
500	ZnAc	1.71 ± 0.16 mm	1.64 ± 0.11 mm	1.82 ± 0.09 mm	1.79 ± 0.07 mm	1.86 ± 0.12 <sup>a</sup> mm
	ZnCl <sub>2</sub>	1.37 ± 0.13 mm	1.35 ± 0.14 mm	1.35 ± 0.10 mm	1.37 ± 0.15 mm	1.38 ± 0.06 <sup>a</sup> mm
1000	ZnAc	1.94 ± 0.04 mm	1.90 ± 0.13 mm	2.01 ± 0.23 <sup>ab</sup> mm	2.00 ± 0.10 mm	2.08 ± 0.03 <sup>b</sup> mm
	ZnCl <sub>2</sub>	1.39 ± 0.18 <sup>b</sup> mm	1.36 ± 0.08 mm	1.39 ± 0.12 <sup>b</sup> mm	1.38 ± 0.09 mm	1.40 ± 0.10 <sup>b</sup> mm

Values are mean ± SD for three determinations

<sup>a</sup>Significantly ( $p < 0.05$ ) higher compared at the same concentration in each row

<sup>b</sup>Significantly ( $p < 0.05$ ) higher compared at the same concentration in each column

nanoaggregates from zinc chloride and zinc acetate respectively. All the observed peaks were similar to previous findings reported by Dobrucka and Dugaszewska [41].

#### 4.3 SEM and TEM analysis

From the results, both samples show an aggregation of particles ( $\times 5000$  magnification) with spherical and flake-like structures for ZnO nanostructures synthesized from zinc acetate and zinc chloride respectively. The flake-like morphology was formed from an agglomeration of nano-rods as in the TEM image (Fig. 2d). The particle size determined for the nanospheres was approximately 107 nm whereas the length, width, and average mean size of the nanorods as per the TEM analysis was 167 nm, 68 nm, and 206 nm. Similar observations

were recorded in a study by Droepenu et al. [34], Gopal and Kamila [42], Rao and Guatam [43], Zheng et al. [44], and Tripathi et al. [45].

#### 4.4 EDX analysis

EDX results of aqueous extract of *A. occidentale*-mediated ZnO NPs synthesized using zinc acetate and zinc chloride as precursors are shown in Fig. 3. The analysis confirmed the presence of oxide form of zinc nanoparticles with percent mass of Zn and O at 67.09% and 18.66% for sample synthesized from zinc acetate precursor and 64.23% and 17.36% for samples synthesized from zinc chloride respectively. The carbon content present might be due to the basic component of plant materials. The result obtained in this study could be said to be

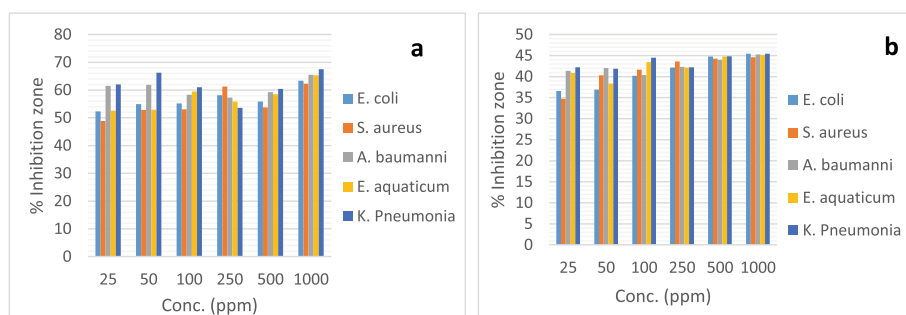


**Fig. 5** Comparative antibacterial evaluation of *A. occidentale* leaf extract-mediated biosynthesized ZnO nanoaggregates from **a** ZnAc and **b** ZnCl<sub>2</sub> precursors for selected microbes

almost in conformity with the study by Mohammadi-Aloucheh et al. [46].

#### 4.5 UV-vis analysis

The distinct absorption peak of the UV-vis analysis for ZnO nanocrystals synthesized using zinc acetate dihydrate and zinc chloride precursor for *A. occidentale* are observed at 360.90 and 362.80 nm respectively. According to Gupta et al. [47], the adsorption edge shifts to lower wavelength as the particle size decreases. Wavelength for the two samples in this study decreased from 362 to 360 nm corresponding to the decrease in particle size from 206 to 107 nm. Literature also shows that absorption depends on factors such as band gap, oxygen deficiency, size and structure of the nanoparticles, surface nature, and impurity centers [48]. These factors could affect the blue-shift of the absorption peak due to the reduction of the particle size [49] as revealed by the TEM analysis. Similar studies reported the absorption band for ZnO nanocrystals in the range of 355–380 nm [50–52].

#### 4.6 Antibacterial activity analysis

Significant differences existed between the two ZnO nanoaggregates and the microbes under study. From the results, ZnO nanoaggregates using zinc acetate dihydrate as precursor were more effective than the one from zinc chloride precursor ( $p > 0.05$ ). Generally, zone of inhibition increased with increase concentration of the two extracts for all microbes as in Table 2 and Fig. 5 a and b. Irregularity in this trend occurred mostly in the 250 ppm and 500 ppm for *A. baumannii*, *E. aquaticum*, and *K. pneumonia*. At a concentration of 1000 ppm for *K. pneumonia*, ZnO nanocrystals from zinc acetate precursor showed maximum antibacterial activity of 67.53% (2.08 mm) as compared to that of zinc chloride at the same concentration (Fig. 5a) with an activity of 45.45% (1.40 mm) with reference to the control used. Commercial synthesized ZnO NPs (Sigma–Aldrich, USA) containing the same volume of methanol was used as control to identify the activity of the solvent and ZnO nanoparticle. On the other hand, the least antibacterial activity (zone of inhibition) was recorded for *S. aureus* with 34.75% (1.06 mm) and 48.85% (1.49 mm) by extract using zinc chloride and zinc acetate dihydrate precursors respectively at concentration of 25 ppm (Fig. 5b). The presence of high concentration of bioactive ingredients especially tannins in *A. occidentale* leaf from literature could probably account for the high antibacterial activities against the microbes used in this study. Variations in the activity of the two ZnO nanocrystals with the same active ingredients in the extract could be associated with the particle sizes of the two samples [53, 54] and the organic nature of the precursor, zinc acetate dihydrate which binds

perfectly with tannins (polyphenols) for effective precipitation of proteins (microbes). Moreover, the entrapment efficiency determined for the two ZnO NPs using zinc acetate dihydrate and zinc chloride as precursors (89.1% and 87.4%) respectively also accounted for the variations in the activity. Ayepola and Ishola [55] in their study with both aqueous and methanolic extracts of *A. occidentale* leaf reported that methanolic extracts recorded a higher antimicrobial activity against selected pathogens (*B. subtilis*, *K. pneumonia*, and *E. coli*) than the aqueous extract. The reason was that tannins are polyphenols that can bind and precipitate proteins [56], thereby having a broader range of antibacterial activity.

#### 5 Conclusion

Biosynthesis of ZnO nanoaggregates using aqueous extract of *A. occidentale* leaf from zinc acetate dihydrate and zinc chloride as precursors was successful, with nanosphere and nanoflake morphologies and the confirmation of elemental zinc from the EDX analysis for the two samples. Particle size determined for the nanoaggregates using zinc acetate dihydrate and zinc chloride precursors were 107 nm and 206 nm respectively.

The active ingredients present in the leaf plant from literature as well as the zinc nanoparticles have shown positive results in the antibacterial activity of the selected microbes. Based on the results of this study, the following conclusions were drawn:

- Increasing the concentration of the extract in the study increases the zone of inhibition generally for all the pathogens under investigation. Irregularities in this trend occurred in *A. baumannii*, *E. aquaticum*, and *K. pneumonia* for the 250 ppm and 500 ppm concentrations.
- ZnO nanoaggregates synthesized from zinc acetate dihydrate recorded higher antibacterial activity in all the microbes used more than antibacterial activity of ZnO nanoaggregates from zinc chloride precursors.
- ZnO nanoaggregates using zinc acetate dihydrate as precursor gave the highest antibacterial activity of 67.53% (2.08 mm) in *K. pneumonia* at 1000 ppm concentration.
- The least antibacterial activity occurred in *S. aureus* with 34.75% (1.06 mm) zone of inhibition at a concentration of 25 ppm by extract used in synthesizing ZnO nanoaggregates using zinc chloride as precursor.

#### Abbreviations

ZnO: Zinc oxide;  $Zn(CH_3COO)_2 \cdot 2H_2O$ : Zinc acetate dihydrate;  $ZnCl_2$ : Zinc chloride; Gram +ve: Gram positive; Gram –ve: Gram negative; FT-IR: Fourier transform infrared spectroscopy; SEM: Scanning electron microscopy; TEM: Transmission electron microscopy; EDX: Energy-dispersive x-ray



spectroscopy; UV-vis: Ultraviolet visible spectroscopy; OD: Optical density; KBr: Potassium bromide; KOH: Potassium hydroxide; ZnAc: Zinc acetate dihydrate; NPs: Nanoparticles

#### Acknowledgements

The authors acknowledge the contribution of colleagues from Faculty of Resource Science and Technology (FRST) Geochemistry Laboratory and Analytical Laboratory, Universiti Malaysia Sarawak; Department of Pharmaceutics, Phytochemistry Laboratory, Centre for Plant Medicine Research, Mampong-Akuapem, Ghana; Chemistry Laboratory, Department of Biochemistry Laboratory, University of Ghana-Legon; and Mr. Obeng Wilson, a peasant farmer in Dormaa Ahenkro in the Brong Ahafo region of Ghana.

#### Authors' contributions

MOK and FA undertook formal identification and collection of the plant species. EKD, AEA, BSW, and RBW designed the research. MOK, FA, EKD, BSW, RBW, and AEA conducted the review and editing. Centre for Plant Medicine Research, Mampong-Akuapem, Ghana, provided resources. EKD and AEA wrote the paper. Finally, all authors have read and approved the manuscript for publication.

#### Funding

The authors received no specific funding for this work.

#### Availability of data and materials

The dataset used during the current study are available from the corresponding author on reasonable request.

#### Ethics approval and consent to participate

Not applicable

#### Consent for publication

Not applicable

#### Competing interests

The authors declare that they have no competing interests.

#### Author details

<sup>1</sup>Resource Chemistry Program, Faculty of Resource Science and Technology, Universiti Malaysia Sarawak, 94300 Kota Samarahan, Sarawak, Malaysia.

<sup>2</sup>Graduate School of Nuclear and Allied Sciences, University of Ghana, AE1, Kwabenya, Accra, Ghana. <sup>3</sup>Department of Pharmaceutics, Centre for Plant Medicine Research, Mampong-Akuapem, Ghana. <sup>4</sup>Department of Phytochemistry, Centre for Plant Medicine Research, Mampong-Akuapem, Ghana.

Received: 6 March 2020 Accepted: 12 December 2020

Published online: 06 January 2021

#### References

- Gnanajobitha G, Paulkumar K, Vanaja M (2013) Fruit-mediated synthesis of silver nanoparticles using *Vitis vinifera* and evaluation of their antimicrobial efficacy. *Nanostructure Chemistry* 3(67):1–6
- Duran N, Marcato PD, Alves OL (2005) Mechanistic aspects of biosynthesis of silver nanoparticles by several *Fusarium oxysporum* strains. *Nanotechnology* 3:1–7
- Ingle A, Gade A, Pierrat S (2008) Mycosynthesis of silver nanoparticles using the fungus *Fusarium acuminatum* and its activity against some human pathogenic bacteria. *Current Nanoscience* 4:141–144
- Taylor PL (2005) Usher AL, Burrell RE. Impact of heat on nanocrystalline silver dressings. Part I: chemical and biological properties. *Biomaterials* 26: 7221–7229
- Yang M, Pang G, Jiang L, Feng S (2005) Hydrothermal synthesis of one-dimensional zinc oxides with different precursors. *Nanotechnology* 17:206–212
- Hasanpoor M, Aliofkhaezrai M, Delavari H (2015) Microwave-assisted synthesis of zinc oxide nanoparticle. 5<sup>th</sup> International Biennial Conference on Ultrafine Grained and Nanostructured Materials, UFGNSM15. *Procedia Material Science* 11:320–325
- Xu HY, Wang H (2004) Hydrothermal synthesis of zinc oxide powders with controllable morphology. *Ceramics International* 30:93–97
- Kiliç B, Gür E, Tüzemen S (2012) Nanoporous ZnO photoelectrode for dyesensitized solar cell. *J Nanomater* DOI: <https://doi.org/10.1155/2012/474656>
- Li B, Wang Y (2011) Hierarchically assembled porous ZnO microstructures and applications in a gas sensor. *Superlattice Microst* 49:433–440
- Vimala K, Sundarraj S, Paulpandi M, Vengatesan S, Kannan S (2013) Green synthesized doxorubicin loaded zinc oxide nanoparticles regulate the Bax and Bcl-2 expression in breast and colon carcinoma. *Process Biochem* 49: 160–172
- Venkatachalam P, Jayaraj M, Manikandan R, Geetha N, Rene ER, Sharma NC et al (2016) Zinc oxide nanoparticles (ZnO NPs) alleviate heavy metal-induced toxicity in *Leucaena leucocephala* seedlings: a physiochemical analysis. *Plant Physiol Biochem* 110:59–69
- Elumalai K, Velmurugan S (2015) Green synthesis, characterization and antibacterial activities of zinc oxide nanoparticles from the leaf extract of *Azadirachta indica* (L.). *Applied Surface Science* 345:329–336
- Matinise N, Fuku XG, Kaviyarasu K, Mayedwa N, Maaza M (2017) ZnO nanoparticles via *Moringa oleifera* green synthesis: physical properties and mechanism of formation. *Applied Surface Science* 406:339–347
- Mohamad NAN, Arham NA, Jai J, Hadi A (2014) Plant extract as reducing agent in synthesis of metallic nanoparticles: a review. *Advanced Materials Research* 832(2014):350–355
- Dubey SP, Lahtinen M, Sarkka H, Sillanpaa M (2010) Bioprospective of *Sorbus aucuparia* leaf extract in development of silver and gold nanocolloids. *Colloids Surf B* 80(2010):26–33
- Christensen L, Vivekanandhan S, Misra M, Mohanty AK (2011) Biosynthesis of silver nanoparticles using *Murraya koenigii*: an investigation on the effect of broth concentration in reduction mechanism and particle size. *Advanced Materials Letters* 2(2011):429–434
- Dwivedi AD, Gopal K (2010) Biosynthesis of silver and gold nanoparticles using *Chenopodium album* leaf extract. *Colloids and Surf A* 369(2010):27–33
- Sathishkumar M, Sneha K, Yun Y-S (2010) Immobilization of silver nanoparticles synthesized using *Curcuma longa* tuber powder and extract on cotton cloth for bactericidal activity. *Bioresource Technology* 101(2010): 7958–7965
- Michiels JA, Kevers C, Pincemail J, Defraigne JO, Dommes J (2012) Extraction conditions can greatly influence antioxidant capacity assays in plant food matrices. *Food Chem* 130(2012):986–993
- Gunalana S, Sivaraja R, Rajendran V (2012) Green synthesized ZnO nanoparticles against bacterial and fungal pathogens. *Program of Natural Science Material International* 22(6):693–700
- Akinpelu DA (2001) Antimicrobial activity of *Anacardium occidentale* bark. *Fitoterapia* 72:286–287
- Doss VA, Thangavel KP (2011) Antioxidant and antimicrobial activity using different extracts of *Anacardium occidentale* L. *International Journal of Applied Biology and Pharmaceutical Technology* 2:436–443
- Souza NC, Oliveira JM, Morrone MS, Albanus RD, Amarante MSM, Camillo CS, Langassner SMZ, Gelain DP, Moreira JCF, Dalmolin RJS, Pasquali MAB (2017) Antioxidant and anti-inflammatory properties of *Anacardium occidentale* leaf extract. Evidence-Based. *Complementary and Alternative Medicine Article ID 2787308*, 8 pages.
- Dahake AP, Joshi VD, Joshi AB (2009) Antimicrobial screening of different extract of *Anacardium occidentale* Linn. leaves. *Interdisciplinary Journal of Contemporary Research in Business* 1:856–858
- Varghese J, Tumkur VK, Ballal V, Bhat GS (2013) Antimicrobial effect of *Anacardium occidentale* leaf extract against pathogens causing periodontal disease. *Advances in Bioscience and Biotechnology* 4:15–18
- Srisawat S, Teanpaisan R, Wattanapiromsakul C, Worapamorn W (2005) Antibacterial activity of some Thai plants against *Porphyromonas gingivalis*. *International Association for Dental Research, 20th Southeast Asia Division & Southeast Asia Association for Dental Education, 16th Annual Scientific Meeting, Malacca* 1–4
- Ojezele MO, Agunbiade S (2013) Phytochemical constituents and medicinal properties of different extracts of *Anacardium Occidentale* and *Psidium Guajava*. *Asian Journal of Biomedical and Pharmaceutical Sciences* 3(16):20–23
- Fadeyi OE, Olatunji GA, Ogundele VA (2015) Isolation and characterization of the chemical constituents of *Anacardium occidentale* cracked bark. *Nat Prod Chem Res* 3(5):1000192
- Bastos TM, Russo HM, Moretti NS, Schenkman S, Marcourt L, Gupta MP, Wolfender J-L, Queiroz EF, Soares MBP (2019) Chemical constituents of

- Anacardium occidentale* as inhibitors of *Trypanosoma cruzi* Sirtuins. *Molecules* 24:1299
30. Heny DS, Philip D, Mathew J (2013) Synthesis of platinum nanoparticles using dried *Anacardium occidentale* leaf and its catalytic and thermal applications. *Spectrochimica Acta Part A: Molecular and Biomolecular Spectroscopy* 114:267–271
  31. Droepenu EK, Asare EA (2019) Morphology of green synthesized ZnO nanoparticles using low temperature hydrothermal technique from aqueous *Carica papaya* extract. *Nanoscience and Nanotechnology* 9(1):29–36
  32. Trease GE, Evans WC (1989). *Pharmacognosy*. 13th. ELBS/Bailliere Tindall, London. 345-346, 535-536, 772-773.
  33. Moazzen MAM, Borghei SM, Taleshi T (2012) Change in the morphology of ZnO nanoparticles upon changing the reactant concentration. *Appl Nanosci* 3:295–302
  34. Droepenu EK, Boon SW, Chin SF, Kuan YK, Zaini BA, Asare EA (2019) Comparative evaluation of antibacterial efficacy of biological synthesis of ZnO nanoparticles using fresh leaf extract and fresh stem-bark of *Carica papaya*. *Nano Biomed Eng* 11(3):264–271
  35. Umaru IJ, Badruddin FA, Assim ZB, Umaru HA (2018b) Antibacterial and cytotoxic actions of chloroform crude extract of *Leptadenia hastata*(pers)Decnee. *Clinical Medical Biochemistry* 4:1–4
  36. Umaru IJ, Badruddin FA, Assim ZB, Umaru HA (2018) Antimicrobial properties of *Leptadenia hastata*(pers)decne leaves extract. *International Journal of Pharmacy and Pharmaceutical Sciences* 10(2):149–152
  37. Sharmila G, Thirumarimurugan M, Muthukumaran C (2019) Green synthesis of ZnO nanoparticles using *Tecoma castanifolia* leaf extract: characterization and evaluation of its antioxidant, bactericidal and anticancer activities. *Microchemical Journal* 145:578–587
  38. Sharma H, Kumar K, Choudhary C, Mishra PK, Vaidya B (2016) Development and characterization of metal oxide nanoparticles for the delivery of anticancer drug. *Artificial cells, nanomedicine, and biotechnology* 44(2):672–679
  39. Jain P, Singh SK, Sharma HP, Basri F (2014). Phytochemical screening and antifungal activity of *Semecarpus anacardium* L. (an anti-cancer plant). *Int. J. Pharm. Sci. Res. (IJPSR)*, 5(5), 1884-1891.
  40. Socrates G (2001) *Infrared and Raman characteristic group frequencies, tables and charts*, 3rd edn. Wiley, Ltd. Chichester. New York. Weinheim. Toronto. Brisbane. Singapore
  41. Dobrucka R, Dugaszewska J (2015) Biosynthesis and antibacterial activity of ZnO nanoparticles using *Trifolium pratense* flower extract. *Saudi J Biological Sci* 23(4):517–523
  42. Gopal VVR, Kamila S (2017) Effect of temperature on the morphology of ZnO nanoparticles: a comparative study. *Applied Nanoscience* 7(3-4):75–82
  43. Rao MD, Guatam P (2016) Synthesis and characterization of ZnO nanoflowers using *Chlamydomonas reinhardtii*: a green approach. *Environ Prog Sustain Energy*:1–7
  44. Zheng Y, Fu L, Han F, Wang A, Cai W, Yu J, Yang J, Peng F (2015) Green biosynthesis and characterization of zinc oxide nanoparticles using *Corymbia citriodora* leaf extract and their photocatalytic activity. *Green Chemistry Letters and Reviews* 8(2):59–63
  45. Tripathi RM, Bhadwal AS, Gupta RK, Singh P, Shrivastav A, Shrivastav BR (2014) ZnO nanoflowers: novel biogenic synthesis and enhanced photocatalytic activity. *J Photochem Photobiol B Biol* 141:288–295
  46. Mohammadi-Aloucheh R, Habibi-Yangjeh A, Bayrami A, Latifi-Navid S, Asadi A (2018) Enhanced anti-bacterial activities of ZnO nanoparticles and ZnO/CuO nanocomposites synthesized using *Vaccinium arctostaphylos* L. fruit extract. *Artificial Cells Nanomedicine and Biotechnology* 46(1):1200–1209
  47. Gupta A, Srivastava P, Bahadur L, Amalnerkar DP, Chauhan R (2014) Comparison of physical and electrochemical properties of ZnO prepared via different surfactant-assisted precipitation routes. *Appl Nanosci* 5(7):787–794
  48. Imran K (2013) Structural and optical properties of Zr doped ZnO nanoparticles. *Opt Mater* 35:1189–1193
  49. Mornani EG, Mosayebian P, Dorrani D, Behzad K (2016) Effect of calcination temperature on the size and optical properties of synthesized ZnO nanoparticles. *Journal of Ovonic Research* 12(2):75–80
  50. Yung MMN, Mouneyrac C, Leung KMY (2014) Ecotoxicity of zinc oxide nanoparticles in the marine environment. *Encyclopedia of Nanotechnology*: 1–17
  51. Talam S, Karumuri SR, Gunnam N (2012) Synthesis, characterization, and spectroscopic properties of ZnO nanoparticles. *ISRN Nano Article ID 372505*: 1–6
  52. Akhil K, Khan SS (2017) Effect of humic acid on the toxicity of bare and capped ZnO nanoparticles on bacteria, algal and crustacean systems. *J Photochem Photobiol B* 167:136–149
  53. Shah M, Fawcett D, Sharma S, Tripathy SK, Poinern GEJ (2015) Green synthesis of metallic nanoparticles via biological entities. *Materials* 8(11): 7278–7308
  54. Stankic S, Suman S, Haque F, Vidic J (2016) Pure and multi metal oxide nanoparticles: synthesis, antibacterial and cytotoxic properties. *J Nanobiotechnol* 14(1):73
  55. Ayepola OO, Ishola RO (2009) Evaluation of antimicrobial activity of *Anacardium occidentale* L. *Advances in Medical and Dental Sciences* 3:1–3
  56. Chung KT, Wong TY, Huang YW, Lin Y (1998) Tannins and human health: a review. *Critical Reviews in Food Science and Nutrition*. 38:421–464

### Publisher's Note

Springer Nature remains neutral with regard to jurisdictional claims in published maps and institutional affiliations.

Submit your manuscript to a SpringerOpen<sup>®</sup> journal and benefit from:

- Convenient online submission
- Rigorous peer review
- Open access: articles freely available online
- High visibility within the field
- Retaining the copyright to your article

Submit your next manuscript at ► [springeropen.com](https://www.springeropen.com)